

Finite element modelling of solidification phenomena

K N SEETHARAMU¹, R PARAGASAM¹,
GHULAM A QUADIR¹, Z A ZAINAL¹, B SATHYA PRASAD²
and T SUNDARARAJAN²

¹School of Mechanical Engineering, Universiti Sains Malaysia, Perak Branch
Campus, 31750 Tronoh, Malaysia

²Department of Mechanical Engineering, Indian Institute of Technology,
Chennai 600 036, India

e-mail: kNSEETHARAMU@hotmail.com

Abstract. The process of solidification process is complex in nature and the simulation of such process is required in industry before it is actually undertaken. Finite element method is used to simulate the heat transfer process accompanying the solidification process. The metal and the mould along with the air gap formation is accounted in the heat transfer simulation. Distortion of the casting is caused due to non-uniform shrinkage associated with the process. Residual stresses are induced in the final castings. Simulation of the shrinkage and the thermal stresses are also carried out using finite element methods. The material behaviour is considered as visco-plastic. The simulations are compared with available experimental data and the comparison is found to be good. Special considerations regarding the simulation of solidification process are also brought out.

Keywords. Casting; solidification; heat transfer; thermal stress; finite element method.

1. Introduction

Most foundries and machining operations have stories about casting which flew into pieces with a bang when being machined, or even when simply standing on the floor! It is easy to dismiss such stories. However, they should be viewed as warnings. They warn that, under certain conditions, castings can have such high stresses locked inside that they are dangerous and unfit for service. We are unaware that the casting may be on the brink of catastrophic failure because, of course, the problem is invisible; the casting looks perfect (Campbell 1991). Over US \$50 M is attributed to thermal stresses generated defects in castings which can be essentially eliminated through the application of computer predictions.

If the castings were to be cooled at a uniform rate and with uniform constraints acting at all points over its surface, it would reach room temperature perfectly in proportion, maybe

a little larger or smaller than required, but not distorted. In practice, of course, this Utopia is never realized. Usually, the casting is somewhat larger or smaller, and is not as accurate a shape as a discerning customer would prefer. Occasionally, it may be very seriously distorted.

Again, wishing ourselves in Utopia, we can envisage that if the constraint by the mould were either zero or infinite, the casting would be of predictable size and correct shape in both cases.

Even if the castings were subjected to no constraint at all from the mould, it would certainly suffer from internally generated constraints as a result of uneven cooling. A well-known example of this effect is the mixed-section casting shown in figure 1. If a failure occurs, it always happens in the thicker section. This may at first sight be surprising. The explanation of this behaviour requires careful reasoning. First, the thin section solidifies and cools. Its contraction along its length is easily accommodated by the heavier section, which simply contracts under the compressive load since it is hot, and therefore plastic, if not actually still molten. Later, however, when the thin section has practically finished contracting, the heavier section starts to contract. It is unable to compress the thin section, which has now become rigid and strong. Thus, the heavy section goes into tension. Depending on its temperature it will stretch plastically, or hot tear, or cold crack.

The example shown in figure 1 is another common failure mode. The internal walls of the castings remain hot longest even though the casting may have been designed with even wall sections. This is, of course, simply the result of the internal sections being surrounded by other hot sections. The reasoning is therefore the same as that for the thick/thin-section casting above. The internal walls of the casting suffer tension at a late stage of cooling. This tension may be retained as a residual stress in the finished casting, or may lead to catastrophic failure by tearing or cracking. The same reasoning applies to the case of a single-component heavy-section casting such as an ingot, billet or slab, especially when these are cast in steel because of its poor thermal conductivity. The inner parts of the

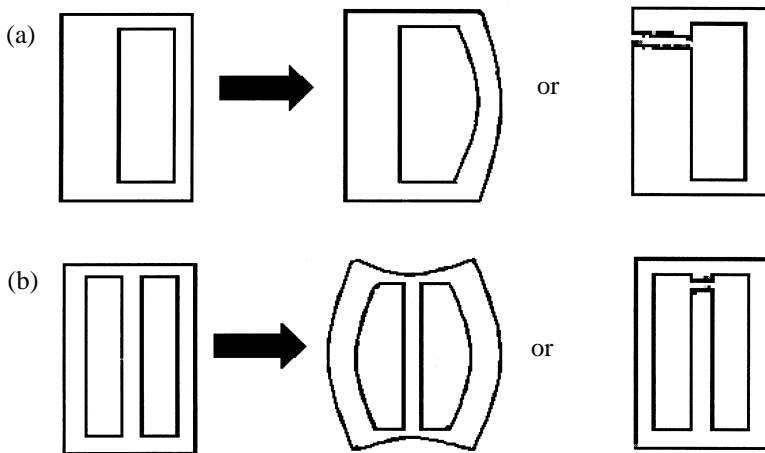


Figure 1. (a) A thick/thin section casting showing tensile stress in the thick section. (b) An even-walled casting showing internal tensile stresses.

casting solidify and contract last, putting the internal parts of the casting into tension. Because of the low yield point of the hot metal, extensive plastic yielding occurs. Further influence of the geometry of the three-bar frame casting was found by Steiger (1913). He measured the increase of the stress in the centre bar of grey iron castings by increasing the rigidity of the end cross members. Also he found that a centre bar of more than twice the diameter of the outer bars would suffer a residual stress of over 200 MPa, which was sufficient to fracture the bar during cooling.

As with cases of the constraint of the casting by the mould, removing the casting from the mould at an early stage would be expected to be normally beneficial in reducing residual stress. Figure 2 shows the result for iron and a high-strength aluminium alloy.

Stress analysis of castings poses several difficulties not seen in more traditional problems in mechanics. The residual stress formation during castings is a consequence of various regions of a geometrically complicated casting cooling at different rates. Stress response is the result of coupled thermal, microthermal and stress histories. Stress predictions are strongly influenced by the thermal and microstructural histories. The accuracy of thermal and microstructural predictions is a primary factor in the accuracy of residual stress predictions.

Figure 3 is a schematic representation of the types of analyses required to completely describe a casting process (Overfelt 1992). An overall architecture of a comprehensive solidification modelling system is shown in figure 4. This figure depicts the various modules available in the current state-of-the-art solidification simulation of casting processes, the information available from each module and the interconnection between each module (Upadhy & Paul 1994).

The primary and most obvious phenomenon controlling casting is the transfer of heat from the cooling metal to the mould. The early models of cooling of casting were straightforward heat conduction analysis. However, the mechanics of fluid flow are important for both mould-filling effects and physics based models of inter-dendritic porosity formation. Buoyancy effects, after the mould is full, exert varying degrees of influence during the cooling cycle depending on the thickness of the casting being produced. In addition, the analysis of the flow of various chemical species is very important for crystal growth and many thermo-fluid models today incorporate species flow.

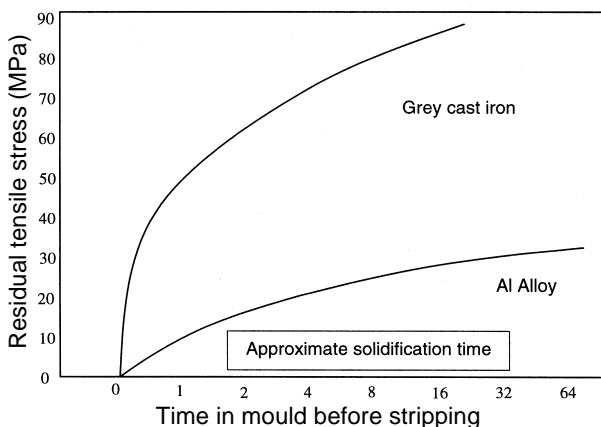


Figure 2. Residual stresses in aluminium alloy and grey iron castings as a function of stripping time.

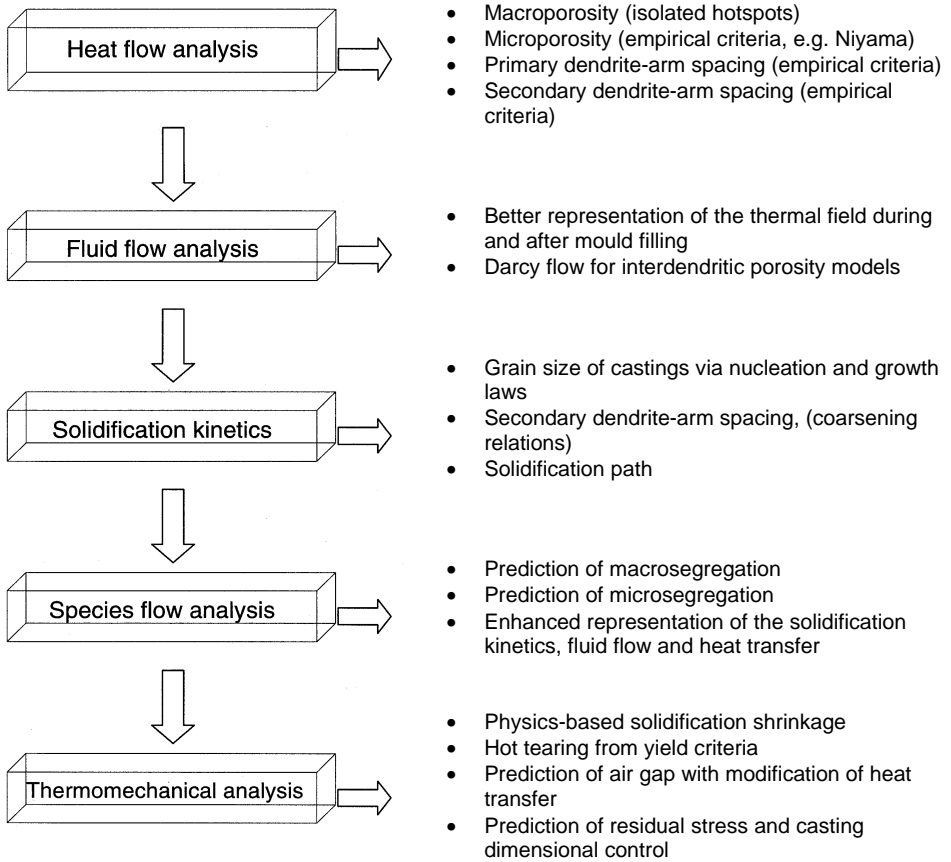


Figure 3. Types of analysis available for solidification modelling and their benefits.

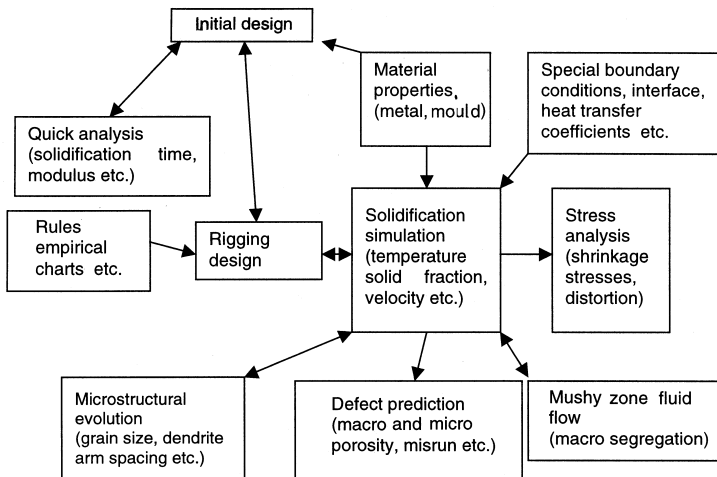


Figure 4. Typical architecture of a comprehensive solidification modelling system.

The heat transfer processes occurring are complex, the cooling rates employed range from 10^{-5} to 10^{10} K/s and the corresponding solidification systems extend from several metres to a few micrometres. These various cooling rates produce different microstructures and hence a variety of thermomechanical properties. Yu *et al* (1992) related the occurrence of casting defects to cooling rates. During the solidification of binary and multi-component alloys the concentrations vary locally from the original mixture as material may be preferentially incorporated or rejected at the solidification front. The material between the solidus and the liquidus temperatures is partly solid and partly liquid and resembles a porous medium and is referred to as 'mushy zone'. Lewis *et al* (1997) have given an account of several aspects of modelling of heat transfer, fluid flow and thermodynamics in castings.

Solidification kinetics including phase selection, nucleation and growth are now being investigated in several laboratories. The incorporation of these principles into the more traditional thermo-fluid models promises to enable quantitative microstructural predictions in the near future (Yu *et al* 1992), and predictions of engineering properties such as tensile strength and elongation will be possible before long. These predictions will enable product-design engineers to evaluate the effects of non-uniform properties and defects on the life cycle performance of components. Finally, the coupling of mechanical analysis with thermal analysis enables the predictions of residual stresses and distortions in castings.

Another important problem is the material response to the thermal cycle as material properties are temperature-dependent (Williams *et al* 1979). For steels and other materials there can be dramatic changes in mechanical properties at temperatures above 600°C. Phase transformations, with their attendant volume changes also play an important role in development of residual stresses.

Thermo-mechanical models were first applied to modelling of continuous casting and ingot casting. Elasto-plastic (Grill *et al* 1976; Kelly *et al* 1988; Guan & Sahm 1992) and elasto-viscoplastic (Fjaer & Mo 1990; Inoue & Ju 1992; Thomas *et al* 1988) behaviours have been considered with thermo-dependent material properties. The effect of different kinds of constitutive equations has been discussed (Kowolowski *et al* 1992) and elasto-viscoplastic behaviour seems to be more appropriate to model the development of strain and stress in casting and to take into account the different states of metal (liquid, semi-solid, solid). Such models were recently applied to the castings of complex shape parts (Shapiro *et al* 1993; Bellet *et al* 1993).

The focus is currently on the validation of models: Do they correctly describe reality and what must be the accuracy of the data materials for models to be predictive? The great influence of thermal properties of alloys on calculated solidification time have been pointed out (Overfelt 1993). And coupling between thermal and mechanical behaviour magnifies the complexity of this problem since not only thermal and mechanical properties must be accurately known but the way the coupling is modeled is of importance.

Chandra (1995) presents the basic concepts for a comprehensive finite element based computer simulation method for the prediction of hot tears, hot cracks, residual stresses and distortions in precision castings using a sequential thermo-mechanical analysis approach. The existing capabilities of several industry standard commercial and research finite element codes are also reviewed by Chandra (1995). Drezer *et al.* (1995) predict the deformation and temperature field evolution during direct chill (DC) and electromagnetic

(EM) casting of aluminium alloy slabs using transient thermo mechanical model based on viscoplastic law. The model is validated on the basis of the measurements. The model enables the prediction of the influence of casting parameters on butt curl and swell, rolling faces and residual stress state for DC and EM cast ingots.

Stefanescu (1995) has made an attempt to predict features like micro segregation, microstructure length scale, and fraction of phases, structural transitions, hardness, microhardness and tensile properties. Distribution of residual porosity in castings is calculated based on a uniform solidification assumption for particular case of aluminium-rich Al–Cu casting (Kuznetsov & Vafai 1995). An analytical criterion, identifying conditions under which there will be no porosity formation, is established (Kuznetsov & Vafai 1995). Heiber *et al* (1994) showed that the strength properties of in situ solidified steel near solidus temperature can be readily determined and hence, may allow to develop a stress criterion in order to further improve the assurance of inner soundness even under most critical conditions. However, Yamanaka *et al* (1995) found that internal cracking occurs and extends when the total amount of strain applied between zero strength (ZST) and zero ductility temperature (ZDT) exceeds the critical strain, independent of deformation mode, whether continuous and intermittent. It is interesting to note that Zhang *et al* (1994) have presented a fast-acting simultaneous filling and solidification model based on reduction of Navier–Stoke equations to transient Bernoulli equation and potential equation along with enthalpy method with 1-D heat conduction model. Ruiz & Khandia (1995) have used LS-DYNA 3D both for the filling simulation and to carry out a coupled thermal and stress analysis of the casting during solidification, predicting cooling rates, residual stresses and as cast shapes. Magnin *et al* (1995) determined the elasto-viscoplastic constitutive equation using an optimization model, which calculates the best rheological parameters to fit experimental stress curves. This law is then introduced in a finite element model of billet DC casting using the commercial software package MARC. A good idea of product quality and performance can often be obtained at the initial stage of the product development cycle by being able to predict filling, solidification, stresses and shrinkage (Hetu *et al* 1995). Examples of simulations conducted using an experimental die, an automotive housing and a wheel in an aluminium alloy are given.

2. Finite element analysis

An experimental on-site study of the influence of the operating parameters on the quality of the casting produced in a working steel mill would be very costly and time-consuming. It is far more practical to simulate the entire complex process numerically and to study the problem by simulation. Any acceptable mathematical model should be capable of accommodating variations in the operating parameters as they arise in practice, so that their effects on the final product can be predicted. Another requirement placed on the model is that it be suitable for designing moulds so that the optimum type of mould may be used for the given casting conditions and steel qualities. Since the entire process is dependent on heat flow from the ingot to the mould and subsequently to the surroundings, it is logical to determine the temperature field at various stages of the process. From this temperature field, initial strains can be calculated and the resulting thermal stresses determined.

Since the appearing of the pioneering paper by Sarjant & Slack (1954) a number of authors have published studies on the development of mathematical models for the calculation of the solidification process in the steel ingots. Although the solidification of an ingot is a three-dimensional process, it appears to be possible to obtain an adequate picture of the process by using a two-dimensional model. It has been demonstrated (Sevrin 1970) that for the ingot dimensions used in actual practice, a true picture of the solidification process can be obtained by calculation in a horizontal section at mid-height through the ingot.

The thermal model used here utilizes the Galerkin method (Lewis *et al* 1996) and eight-noded quadratic isoparametric elements. It possesses the novel feature of using elements with time-varying conductivity to model the heat transfer in the air-gap which forms between ingot and mould. Calculated temperature fields may be used to evaluate the loading stresses, and in this way thermal stress development may be determined using either an elastic (Lewis & Bass 1976) or an elastoplastic formulation (Lewis *et al* 1977). Elastoplastic formulations have the disadvantage of being unable to model any time-dependent creep effects.

The mathematical stress model in this paper embodies a general solution procedure for determining the development of thermal stresses in an elasto-viscoplastic multiphase body and is capable of accounting for time-dependent properties. The constitutive model used is of the type proposed by Perzyna (1966) and first implemented numerically by Zienkiewicz & Corneau (1974). In this model the behaviour of the material is elastic if a certain function of the yield condition has a value which is less than zero, while time-dependent viscoplastic flow occurs when the value of this function is positive. The model can also be used to give the purely plastic solution, in which time and viscous effects do not have their real meanings but are used merely as means for attaining steady-state conditions.

2.1 Finite-element formulation of the heat-flow problem (Morgan *et al* 1981)

The variation of temperature T with time in a two-dimensional region Ω bounded by a curve Γ , for both ingot and the mould is given by the equation,

$$\mathbf{rc} \frac{\partial T}{\partial t} = \frac{\partial}{\partial x} \left(k_x \frac{\partial T}{\partial x} \right) + \frac{\partial}{\partial y} \left(k_y \frac{\partial T}{\partial y} \right), \quad (1)$$

where \mathbf{rc} is the thermal capacity, k_x , k_y are the thermal conductivities in the x , y directions.

The boundary conditions for this partial differential equation are the expressions for the heat fluxes between the ingot and mould and between the mould and the surroundings. These boundaries occur in two regions:

(a) Between ingot and inner wall of the mould,

$$q_{12} = h_{12}(T_1 - T_2) = (k_{12}/d_{12}) (T_1 - T_2) \quad (2)$$

where T_1 is the surface temperature of the ingot, T_2 is the temperature of the inner wall of the mould.

(b) Between outer wall of the mould and the surroundings,

$$q_{3\infty} = h_{3\infty}(T_3 - T_\infty), \quad (3)$$

where T_3 is the temperature of the outer wall of the mould, T_∞ is the ambient temperature.

The heat-transfer coefficient h_{12} changes when the air gap between the ingot and the mould forms. To take this phenomenon into account, h_{12} is regarded as a function of position on the ingot perimeter and of time. Oeters *et al* (1977) have observed that the calculations are in good agreement with the actually measured heat-flow densities in the gap if the breadth of the gap is taken to be of the order of 0.5 mm. Thus in the present model, the heat transfer across the gap is modelled in the conduction mode with conductivity being a function of time and position on the perimeter. This approach allows the effect of the lubrication used on the inner wall of the mould (Oeters *et al* 1977) to be modelled by using a suitable value of the thermal conductivity in the air-gap region. The heat-transfer coefficient between the outer wall of the mould and the surrounding air takes into account heat transfer by radiation and by free convection. The variation of density and specific heat with temperature is handled as discussed by Comini *et al* (1974) and any phase change, which occurs, is treated by the method discussed by Morgan *et al* (1978). The thermal conductivities of the ingot and mould are also allowed to vary with temperature. The temperature fields in the ingot and the mould are computed simultaneously using a finite-element formulation. The region of interest is divided into a number of eight-noded isoparametric elements Ω^e , with boundary Γ^e with quadratic shape functions N_i associated with each node i . In the isoparametric elements the shape functions are used to transform the coordinates (Lewis *et al* 1996), and this enables better representation of any curved boundaries which may be present in the problem. The unknown temperature T is approximated in the solution domain at any time by

$$T = \sum_{i=1}^n N_i T_i(t). \quad (4)$$

where T_i is the time-dependent value at node i . The substitution of (4) into (1) and the application of the Galerkin method (Lewis *et al* 1996) results in the equation,

$$\mathbf{KT} + \mathbf{CT} = \mathbf{F}, \quad (5)$$

in which typical matrix elements are

$$K_{ij} = \sum_e \int_{\Omega^e} \left(K_x \frac{\partial N_i}{\partial x} \frac{\partial N_j}{\partial x} + K_y \frac{\partial N_i}{\partial y} \frac{\partial N_j}{\partial y} \right) d\Omega + \sum_e \int_{\Gamma^e} h N_i N_j d\Gamma, \quad (6)$$

$$C_{ij} = \sum_e \int_{\Omega^e} \rho c N_i N_j d\Omega, \quad (7)$$

$$F_i = - \sum_e \int_{\Gamma^e} N_i h T_\infty d\Gamma, \quad (8)$$

where the summations are carried out over each element e .

The coupled system of ordinary differential equations represented by (5) is solved by a finite-difference two-stage Crank–Nicolson predictor–corrector method and, in this way, the complete thermal history of the region may be determined. The change in the temperature in a certain time can then be used to calculate incremental initial node strains $d\boldsymbol{\varepsilon}_i$ via

$$d\boldsymbol{\varepsilon}_i = \begin{Bmatrix} \mathbf{a}\Delta T_i \\ \mathbf{a}\Delta T_i \\ 0 \end{Bmatrix}, \quad (9)$$

where \mathbf{a} is the temperature–dependent coefficient of expansion. An elasto–viscoplastic stress model is then used to calculate the stress distribution resulting from the application of this initial strain.

2.2 The finite-element formulation of the elasto-viscoplastic stress model (Morgan et al 1981)

In the elasto-viscoplastic stress model it is assumed that the total strain is the sum of elastic and plastic components, together with any initial strains, i.e.

$$\boldsymbol{\varepsilon} = \boldsymbol{\varepsilon}_e + \boldsymbol{\varepsilon}_{np} + \boldsymbol{\varepsilon}_i. \quad (10)$$

Only elastic strains are produced initially by the application of a load, and the elastic strain rate is linearly related to the total stress rate by the matrix of elastic constants \mathbf{D} (Zienkiewicz 1977) according to

$$\dot{\boldsymbol{\sigma}} = \mathbf{D}\dot{\boldsymbol{\varepsilon}}_e \quad (11)$$

where the dot denotes differentiation with respect to time. The viscoplastic strain occurs only if the stress levels exceed some previously defined yield stress. This yield stress is given by the yield function

$$F(\boldsymbol{\sigma}, \boldsymbol{\varepsilon}_{np}) = 0. \quad (12)$$

Therefore when $F < 0$, purely elastic behaviour takes place, but $F > 0$ represents the onset of plastic deformation.

The viscoplastic strain is given by

$$(\partial\boldsymbol{\varepsilon}_{np} / \partial t) = \dot{\boldsymbol{\varepsilon}}_{ip} = f(\dot{\phi} \cdot \boldsymbol{\varepsilon}_{np}). \quad (13)$$

To define completely a strain–rate law, it is assumed that, in common with plasticity, the directions of straining are given by gradients of a plastic potential Q . The viscoplastic flow laws can then be written as

$$\dot{\boldsymbol{\varepsilon}}_{np} = \mathbf{y}(F)(\partial Q / \partial \dot{\phi}), \quad (14)$$

where

$$\mathbf{y}(F) = \begin{cases} 0, & \text{if } F \leq 0, \\ \mathbf{y}(F), & \text{if } F > 0. \end{cases}$$

Combining (10), (11), and (13) results in the complete constitutive relation

$$\dot{\mathbf{a}} = D^{-1}\dot{\mathbf{s}} + \mathbf{y}(F)(\partial Q/\partial \dot{\mathbf{o}}) + \dot{\mathbf{a}}_i. \quad (15)$$

The finite-element stress analysis is performed only on the ingot, which is discretized by using the same elements and shape functions as were used in the thermal analysis. If the vector \mathbf{u} denotes the displacement field, then this may be approximated over in terms of the nodal displacements δ_i by,

$$\mathbf{u} = \tilde{\mathbf{u}} = \sum_{i=1}^n \mathbf{N}_i \tilde{\mathbf{a}}_i = \mathbf{N}^T \tilde{\mathbf{a}}, \quad (16)$$

where δ is the column vector of nodal values δ_i . With the displacements at all points

$$\boldsymbol{\varepsilon} = \mathbf{B}\delta, \quad (17)$$

given by (16) the strains at any point can be determined from the relationship where \mathbf{B} is the standard matrix derived from the derivatives of the shape functions (Zienkiewicz 1977).

The virtual work principle in this case enables the equilibrium equation to be written as

$$\int_{\Omega} \mathbf{B}^T \dot{\mathbf{s}} d\Omega = 0. \quad (18)$$

As the constitutive relation for viscoplastic problems has been specified in time rate form in (11), it is convenient to rewrite (18) as

$$\int_{\Omega} \mathbf{B}^T \dot{\mathbf{s}} d\Omega = 0. \quad (19)$$

Combining (10), (11), and (19) then leads to

$$\int_{\Omega} \mathbf{B}^T \mathbf{D}(\dot{\boldsymbol{\varepsilon}} - \dot{\boldsymbol{\varepsilon}}_{np} - \dot{\boldsymbol{\varepsilon}}_i) d\Omega = 0, \quad (20)$$

which, on using (17) to substitute for $\boldsymbol{\varepsilon}$, becomes

$$\int_{\Omega} \mathbf{B}^T \mathbf{D} \mathbf{B} \dot{\mathbf{a}} d\Omega = 0, \quad (21)$$

i.e.

$$\mathbf{K}_s \dot{\mathbf{a}} - \dot{\mathbf{R}} = 0, \quad (22)$$

where

\mathbf{K}_s is the overall stiffness matrix, $\dot{\mathbf{R}}$ represents the total loading rate,

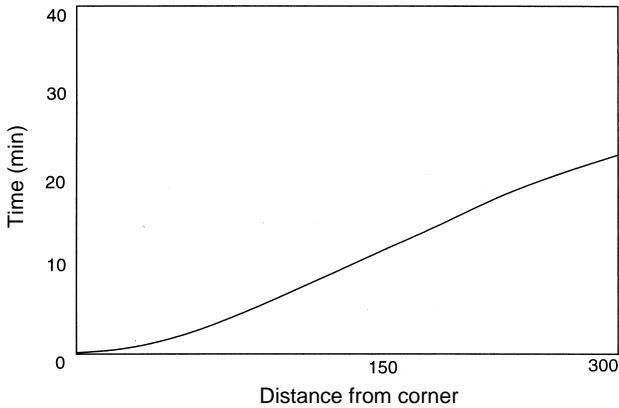


Figure 6. Time for air gap formation.

The time of air-gap formation at various locations on the perimeter of the ingot follows roughly a parabolic law proceeding from the corner to the middle of the face (see figure 6). Initially the model is run with intimate contact everywhere and then the gap opens from the corner towards the centre as time proceeds. In the gap, the heat-transfer coefficient given by Oeters *et al* (1977) are utilized as functions of time in the form shown in figure 7. Since the gap width is fixed at 0.5 mm, this variation is supplied to the model as a variation in thermal conductivity of the air gap. At the start, the time steps need to be very small, of the order of seconds, and they gradually increase up to a value of 2 minutes in the later stages of the simulation run.

The calculated temperature of the inner wall of the mould for various locations is plotted against time (figure 8). For the sake of comparison, the results of Oeters *et al* (1977) are also shown on the same figure. It can be concluded that a reasonable agreement exists in view of the exact thermal properties used by Oeters *et al* (1977) are not known. Figure 9 shows a comparison of surface temperatures on the ingot as functions of time and

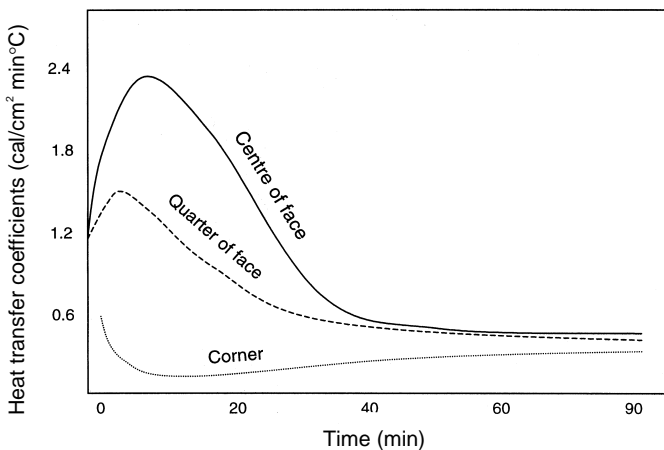


Figure 7. Average heat transfer coefficients in air gap.

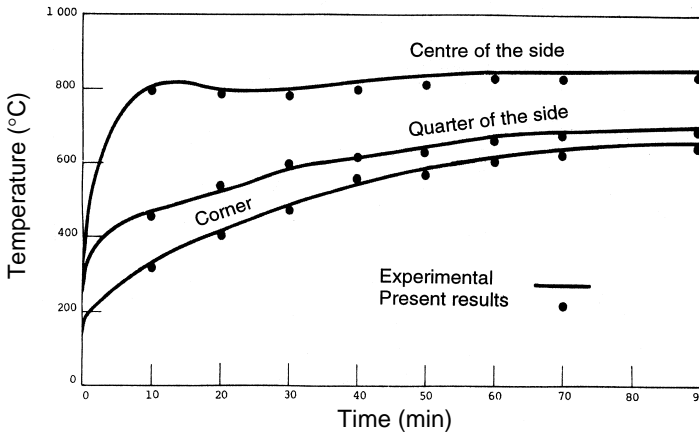


Figure 8. Temperature curve for inner wall of mould.

location. It can be observed that the predicted temperatures are again slightly lower than those of Oeters *et al* (1977). Figure 10 shows the solidification fronts determined at various time intervals; these results are in good agreement with the value determined by Weingert (1968).

The temperature field in the ingot is used for evaluating the thermal loads to be used in the visco-plastic stress analysis. A plane strain stress analysis was performed, using a Von Mises yield criterion (Zienkiewicz 1977). The model is used to give a purely plastic solution at steady-state conditions at each stage. The rate of viscoplastic straining is given by (14), in which the flow function used is

$$f = g(F/F_0), \tag{24}$$

where

F_0 is some reference value of stress, g is a fluidity coefficient.

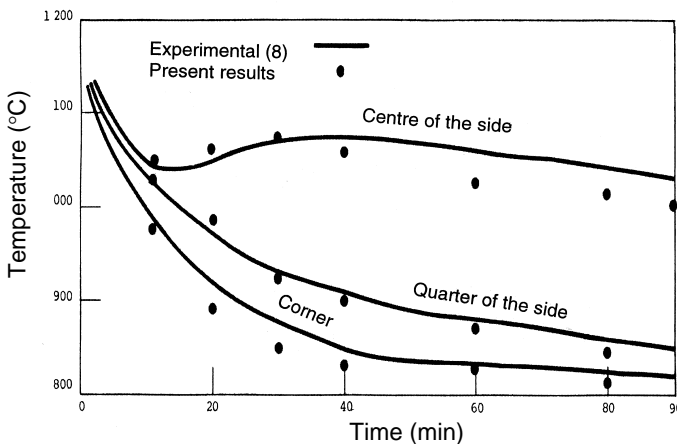


Figure 9. Average value of ingot surface temperature.

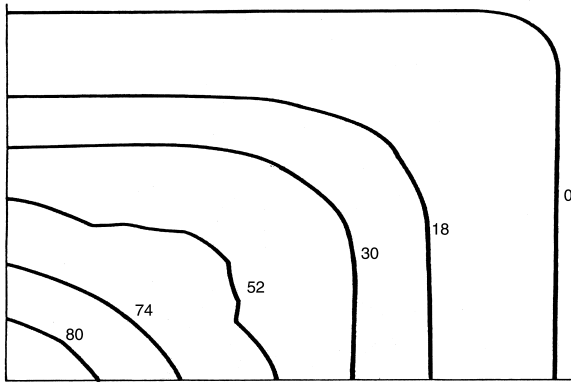


Figure 10. Solidification fronts for one quadrant of the ingot.

The mechanical properties vary as a function of temperature and are taken from Williams *et al* (1979). A Poisson's ratio value of 0.33 is used.

Figures 11 and 12 show the computed stress field in the ingot at two different times. It can be observed from these figures that the region near the ingot surface is subjected to tension initially and that, as expected, this gradually changes to compression with the passage of time. Prediction of such stress concentration regions would be particularly useful in the case of complex shapes to avoid possible failures.

3. Special considerations

Deformation of solidifying material is very different from that of a standard fixed body. A solidifying body develops residual (initial) stresses immediately after solidification and is never in a state of zero stresses (stress free state). Thermal stress problems carry with it difficulties not normally found in the analysis of either thermal or stress problems. Coupling between the temperature and stress fields works in both direction. It is possible to imagine cases, where the basic boundary conditions for the thermal analysis are affected

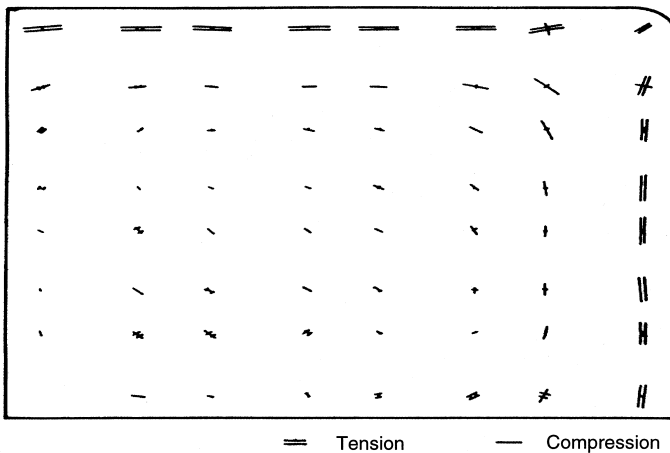


Figure 11. One quadrant of the principal stress field after four minutes.

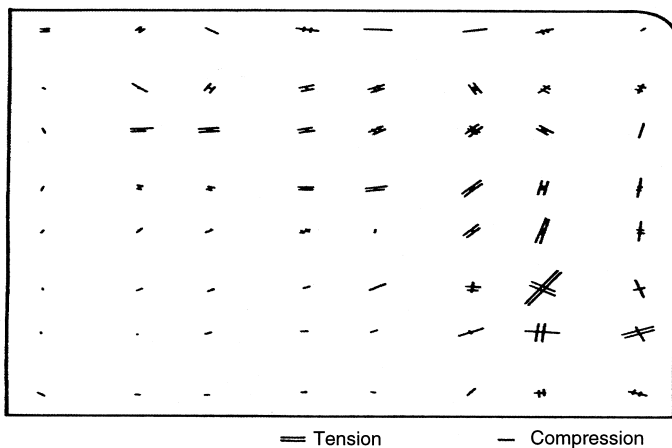


Figure 12. Principal stress field after 40 minutes.

by the deformations as in the formation of the air gap which controls the heat flow to the mould from the cooling ingot. Fully coupled analysis are slightly more complicated because they require decisions to be made about when to update the effect of one process to the other. De Coultieux *et al* (1997) present an application of a 3D finite element coupled thermo-mechanical model to the solidification of a hollow cylinder. An experiment has been developed to measure heat transfer coefficients and air gap widths in permanent mould casting of aluminium–silicon alloys. Comparison between experimental and calculated temperature and air gap width shows the validity of the coupled approach.

Thermal strain fields computed from temperature fields introduce complications. The incompressible nature of plastic deformation creates a constraint at each gauss point in an element. When the number of constraints arising from incompressibility exceeds the numbers of degrees of freedom, locking is said to occur, as there is no possible solution for this case. The solution to this maybe the reduced order of the integration for the hydraulic components of the stress, which may lead to most notably a failure to satisfy the patch test (Oddy & Lindgren 1997). A related effect comes from the order of the thermal strain fields within the element. If nodal temperatures are interpolated to give gauss point values, and these used to determine thermal strains, then the thermal strain field has the same order as the displacement field in the element. The total strains, which are computed from the partial derivatives of the displacements, are one order lower. This incompatibility can also lead to locking problems. The need to avoid incompatible strain fields has been known for sometime (Anderson 1978) and extremely large errors that can result if it is not observed (Oddy *et al* 1990). Using linear elements in the thermal analysis and quadratic elements in the stress analysis is the most common strategy (Nichocals Zabarar *et al* 1991).

The use of plane strain conditions are most commonly used in the stress analysis. This condition implies that the longitudinal heat flow and longitudinal displacement are zero. Longitudinal interactions in the stress may not always be satisfied even though longitudinal heat flow is probably never very large. To compensate for this problem, the extension of this to a generalized plane strain has been used (Oddy & Lindgren 1997) where plane sections must remain plane but may rotate or translate with respect to one another in which case net longitudinal stress on any cross-section now becomes zero.

One of the main purposes of solidification modelling is to identify casting designs that are likely to cause defects due to the porosity formed due to shrinkage during phase change frequently take the form of interdendritic void affects the ultimate tensile strength of casting and hence is to be avoided. The porosity can be eliminated only when the liquid metal from the riser is able to travel to the hot spot location to compensate for the solidification. Experiments on cast steels have shown that when the temperature gradient at the end of the solidification falls to below 10 K/cm, the porosity is observed even in well-degassed material. On the basis of solidification simulation, the solidification time can be found and the temperature gradients at that instant can be determined. Based on the contour of 10 K/cm thermal gradient, it is possible to determine the location and size of the shrinkage defect. However, it may be noted that the value of 10 K/cm is valid for a 3-D casting and a different limit may have to be taken for 2-D simulations. Sathya Prasad (1999) has predicted the size and location of shrinkage cavity for L-shaped and T-shaped castings with and without chills. Residual stress determination must also make sure that no shrinkage cavity exists in the castings. If it exists, its presence must be accounted, as there may be stress concentration around such shrinkage cavity.

In the case of continuous casting of steel, several additional difficulties are encountered while predicting the residual stresses compared to ingot casting. High stresses develop in the solidifying shell as a result of a number of forces acting externally and internally on the strand. The values of heat extraction and solidification are relatively slow for static casting (solidification time measured in hours) where as solidification time for continuous casting is in minutes. A single cooling environment over its solidification period exists for a static casting whereas continuous cast section encounters different environment-mould, sprays, pinch rolls contact, radiation before complete solidification take place. Thus the continuously cast change rapidly from one zone to another resulting in higher thermal stresses than in ingot castings. Continuous cast section, in addition, is also stressed by pinch rolls, bending and straightening operations during solidification mould oscillation, misalignment of mould and roller cages. Ferrostatic pressure can also produce sufficient stress to cause bulging across the wide faces of large slabs.

The effect of size of castings and thermal boundary conditions on the residual stresses and deformation has been investigated by Sathya Prasad (1999). A critical study of the role of material properties on the double-diffusive convection is carried out by simulating solidification of aqueous ammonium chloride, iron-carbon and lead-tin binary systems by Basu & Singh (1997). It is seen that material properties play a very crucial role on the nature of double diffusive convection and consequently on macro segregation. Lewis *et al* (2001) have discussed the formation of residual stresses in castings.

4. Concluding remarks

The finite element method as applied to casting problem is demonstrated in terms of both temperature and stress fields for an ingot casting where the experimental data was available. Special conderations in the modelling of the casting process is also included.

The material presented here is collected from several papers apart from our own work. The authors gratefully acknowledge, the authors and publishers of such papers which we have made use of in preparing this article.

References

- Anderson B A B 1978 Thermal stresses in a submerged-arc welding joint considering phase transformations. *J. Eng. Mater. Technol., Trans. ASME* 100: 356–362
- Basu B, Singh A K 1997 Role and characterization of double diffusive convection during solidification of binary alloys. *Proceedings of the Third ISHMT-ASME Heat and Mass Transfer Conference and Fourteenth National Heat Mass Transfer Conference*, IIT, Kanpur, pp 129–141
- Bellet M, Menai M, Bay F 1993 Finite element modelling of the cooling phase in casting processes. *Modelling of casting, welding and advanced solidification processes VI* (eds) T S Piwonka, V Voller, L Katgermann (The Minerals, Metals and Materials Society) pp 561–568
- Campbell J 1991 *Casting* (London: Butterworth Heinemann)
- Chandra V 1995 Computer predictions of hot tears, hot cracks, residual stresses and distortions in precision castings. Basic concepts and approach. *Proc. 124 TMS Annual Meeting*, Warandale, PA, pp 107–117
- Comini G, del Guidice S, Lewis R W, Zienkiewicz O C 1974 Finite element solution of nonlinear heat conduction problems with special reference to phase change. *Int. J. Numer. Methods Engrg.* 9: 109–127
- Corneau I C 1975 Numerical stability in quasi-static elasto-viscoplasticity. *Int. J. Numer. Methods Engrg.* 9: 109–127
- Decultiex F, Menai M, Bay F, Levailant C, Schmidt P, Svenson I L, Bellet M 1997 Thermomechanical modelling in casting with experimental validation. *Modelling in welding, hot powder forming and casting* (ed.) L Karlsson (Columbus, OH: ASM Int.) pp 291–313
- Drezet J M, Roppaz M, Krahenbuhl Y 1995 Thermomechanical effects during direct chill and electromagnetic castings of aluminium alloys, Part II. Numerical solution. *Proc. 124 TMS Annual Meeting*, Warandale, PA, pp 941–950
- Fjaer H G, Mo A 1990 ALSPEN, A mathematical model for thermal stresses in direct chill casting of aluminium billets. *Metall. Trans.* B21: 1049–1061
- Grill A, Brimacombe J K, Weinberg F 1976 Mathematical analysis of stresses in continuous casting of steel. *Ironmaking Steelmaking* 1: 38–47
- Guan J, Sahn P R 1992 Numerical investigations of thermal stresses in real 3D structural casting. *Gisserei* 8: 318–322
- Heibler H, Zirngast J, Bernhard Ch 1994 Inner crack formation in continuous castings: Stress or strain criterion. *Proc. 77 Steelmaking Conference*, PA, vol. 77, pp 405–416
- Hetu J F, Gao D M, Kabanemi K K, Bergeron S, Nguyen K T, Loong C A 1998 Numerical modelling of casting processes. *Adv. Performance Mater.* 5: 65–82
- Inoue T, Ju D Y 1992 Simulation of solidification and viscoplastic stresses during vertical semi-continuous direct chill casting of aluminium alloys. *Int. J. Plasticity* 8:
- Kelly J E, Michalek K P, O'Connor T G, Thomas B G, Dantzig J A 1988 Initial development of thermal and stress fields in continuous cast steel billets. *Metall. Trans.* A19: 1589–2602
- Kowalski P F, Thomas B G, Azzi J A, Wang H 1992 Simple constitutive equations for steel at high temperatures. *Metall. Trans.* B23: 903–918
- Kuznetsov V, Vafai K 1995 Development and investigation of three phase model of the mushy-zone for analysis of porosity formation in solidifying castings. *Int. J. Heat Mass Transfer* 38: 2557–2567
- Lewis R W, Bass B R 1976 The determination of temperature and stresses in cooling bodies by finite elements. *ASME Trans., J. Heat Transfer* 98: 478–484
- Lewis R W, Morgan K, Gallagher R H 1977 *Finite element analysis of solidification and welding processes* (ASME)PVP-PB-026, pp 67–80
- Lewis R W, Morgan K, Thomas H R, Seetharamu K N 1996 *The finite element methods in heat transfer analysis* (New York: John Wiley)
- Lewis R W, Seetharamu K N, Prasad B 1997 Modelling of heat transfer, fluid flow and thermodynamics in castings. In *Modelling in welding, hot powder forming and casting* (ed.) L Karlsson (Columbus, OH: ASM Int.) pp 161–273

- Lewis R W, Seetharamu K N, Hassan A Y 2001 Residual stress formation during casting. In *Handbook of residual stress and distortion of steel* (Columbus, OH: ASM Int.) ch. 5
- Margin B, Katgerman L, Hannart B 1995 Physical and numerical modelling of thermal stress generation during DC casting of aluminium alloys. *Proc. 7th Conf. on Modelling of Casting, Welding and Advanced Solidification Processes* (TMC) pp 303–310
- Morgan K, Lewis R W, Zienkiewicz O C 1978 An improved algorithm for heat conduction problems with phase change. *Int. J. Numer. Methods Engrg.* 12: 1191–1195
- Morgan K, Lewis R W, Seetharamu K N 1981 Modelling heat flow and thermal stress in ingot casting. *Simulation* :55–63
- Oddy A S, Lindgren L E 1997 Mechanical modelling and residual stresses. *Modelling in welding, hot powder forming and casting* (ed.) L Karlsson (Columbus, OH: ASM Int.) pp 31–59
- Oddy A S, McDill J M J, Goldak J A 1990 Consistent strain fields in 3D finite elements analysis of welds. *Trans. ASME, Press. Vessel Tech.* 112: 309–311
- Oeters F, Ruttiger K, Selenz H J 1977 Heat transfer in ingot pouring. *Information Symp. On Casting and Solidification of Steel*, Luxembourg, vol. 1, pp 126–167
- Overfelt T 1992 The manufacturing of solidification modelling. *J. Oper. Mainten.* 44: 17–20
- Overfelt T 1993 Sensitivity of a steel plate solidification model to uncertainties in thermophysical properties. *Modelling of casting, welding and advanced solidification processes VI* (eds) T S Piwonka, V Voller, L Katgermann (The Minerals, Metals and Materials Society) pp 663–370
- Perzyna P 1966 Fundamental problems in visco-plasticity. *Adv. Appl. Mech.* 9: 243–377
- Ruiz D J, Khandia Y 1995 Filling and solidification with coupled heat transfer and stress analysis. *Proc. 7th Conf. on Modelling of Casting, Welding and Advanced Solidification Processes* (TMS) pp 991–1006
- Sarjant R J, Slack M R 1954 International temperature distribution on the cooling and reheating of steel ingots. *J. Iron Steel Inst.*: 428–444
- Sathya Prasad B 1999 *Solidification simulation of casting using finite element method*. Ph D thesis, Department of Mechanical Engineering, Indian Institute of Technology, Madras
- Sevrin R 1970 Mathematical study of the thermal evolution of steel ingots. *Mathematical models in metallurgical process developments* (London: Iron & Steel Inst.) pp 147–157
- Shapiro A, Stein W, Raboin P 1993 Casting process modelling using ProCAST and ST2D. *Modelling of casting, welding and advanced solidification processes VI* (eds) S Piwonka, V Voller, L Katgermann (The Minerals, Metals and Materials Society) pp 493–500
- Steiger R V 1913 *Stahl Eisen* 33: 1442
- Stefanescu D M 1995 Methodologies for modelling of solidification, microstructure and stress capabilities. *Iron Steel Inst. Jpn. Int.* 35: 637–650
- Thomas B G, Samarasekera I V, Brimacombe J K 1988 Mathematical model of the thermal processing of steel ingots. *Metall. Trans.* B19: 119–147
- Upadhy G, Paul A J 1994 Solidification modellig. A phenomenological review. *AFS Trans.* :69–80
- Weingert H 1968 *Untersuchungen uber der Temperatur- und Erstarrung-sablanf Schwerer Blocke und Brammen*. Ph D dissertation, Clausthal, Germany
- Williams J R, Lewis R W, Morgan K 1979 An elasto-viscoplastic thermal stress models with application to the continuous casting of metals. *Int. J. Numer. Methods Engrg.* 14: 1–9
- Yamanaka A, Nakajima K, Okamuza K 1995 Critical strain for internal crack formation in continuous casting. *Ironmaking Steelmaking* 22: 508–512
- Yu K O, Nichols J J, Robinson M 1992 Finite element thermal modelling of casting microstructures and defects. *J. Oper. Mainten.* 44: 21–25
- Zabaras N, Ruan Y, Richmond O 1991 On the calculations of deformations and stresses during axially symmetric solidification. *Trans. ASME, J. Appl. Mech.* 58: 865–871
- Zhang Y F, Wang H P, Liu W K 1994 Fast acting simulation of simultaneous filling and solidification. *Transport phenomenon in solidification* (ASME) HTDV 284, pp 215–216
- Zienkiewicz O C 1977 *The finite element method* (London: McGraw Hill)
- Zienkiewicz O C, Cormeau I C 1974 Visco-plasticity, plasticity and creep in elastic solids: A unified numerical solution. *Int. J. Numer. Methods Engrg.* 8: 821–845